Desalination and Water Treatment
www.deswater.com
doi: 10.1080/19443994.2014.910139

54 (2015) 3218–3226
June

Taylor & Francis
Taylor & Francis Group

Characteristic and performance of polyvinylidene fluoride membranes blended with different additives in direct contact membrane distillation

K.C. Chong[a,*], S.O. Lai[a], K.M. Lee[a], W.J. Lau[b], A.F. Ismail[b], B.S. Ooi[c]

[a]*Universiti Tunku Abdul Rahman, Kuala Lumpur Campus, Jalan Genting Kelang, Kuala Lumpur 53300, Malaysia, Tel. +603 4107 9802; email: chongkc@utar.edu.my*
[b]*Advanced Membrane Technology Research Centre (AMTEC), Universiti Teknologi Malaysia, Skudai 81310, Johor, Malaysia*
[c]*School of Chemical Engineering, Engineering Campus, Universiti Sains Malaysia, Seri Ampangan, Nibong Tebal 14300, S.P.S. Pulau Pinang, Malaysia*

Received 15 December 2013; Accepted 21 March 2014

ABSTRACT

Membrane distillation (MD) is a thermal-driven membrane separation process which recently garners interest from academic and industry due to its low energy requirements and the ability to integrate with renewable energy. In this work, two different additives, i.e. polyethersulfone (PES) and ethylene glycol (EG), were added into dope solutions consisting of polyvinylidene fluoride (PVDF) and 1-methyl-2-pyrrolidone (NMP) to prepare membranes for MD applications. The membranes were characterized with respect to thickness, pore size, porosity, and water contact angle using scanning electron microscope and water contact goniometer. Compared with the membranes made from pure PVDF and PVDF–EG system, it is found that PVDF–EG–PES membrane displayed improved characteristics i.e. having optimum porosity, large pore size, and thin membrane thickness coupled with finger-like structure extended from both inner and outer layers of the membrane. In addition to this, the permeate flux of PVDF–EG–PES membrane during MD application was also reported to be the highest among all the membranes studied when tested under same process conditions. With respect to membrane performance stability, the results showed that PVDF–EG–PES membrane could achieve a very consistent permeate flux while maintaining high NaCl rejection throughout 20 h operation, indicating the potential of this membrane in MD process.

Keywords: Membrane distillation; Polyvinylidene fluoride membrane; Surface modification; Polyethersulfone; Permeate flux

1. Introduction

Membrane distillation (MD) is a recent rising membrane separation technology which has been broadly applied in seawater desalination and wastewater treatment from a wide variety of industrial sectors [1]. Unlike pressure-driven membrane processes such as ultrafiltration and reverse osmosis, MD is a thermal-driven process in which the feed water vapor will be transported across the porous hydrophobic membrane by thermal driving force while the liquid permeation will be resisted due to high surface tension [2,3]. As the nature of MD requires relatively low energy to operate, it could be potentially integrated

*Corresponding author.

1944-3994/1944-3986 © 2014 Balaban Desalination Publications. All rights reserved.

with low-grade heat and/or solar energy. Because of this unique feature, MD has thus attracted potential application interest from both academia and industry in recent years [1,3].

The configurations of MD can be generally categorized into direct contact membrane distillation (DCMD), air gap membrane distillation, sweeping gas membrane distillation, and vacuum membrane distillation [1,3]. Of these configurations, DCMD is the simplest MD setup and yet the most heat and mass transfer efficient, mainly due to the occurrence of feed water vapor condensation inside the membrane module. Many research works have been conducted using DCMD due to its simplicity and low energy requirement on laboratory scale in desalination, wastewater treatment, and food processing [1,4–7]. Typical characteristics of a good membrane for MD application shall exhibit high water contact angle value, porous structure with porosity between 35 and 85%, surface pore size of 10 nm–1 μm, and good resistances against harsh chemical and thermal conditions [1]. In order to meet these criteria, hydrophobic materials such as polyvinylidene fluoride (PVDF), polypropylene, and polytetrafluoroethylene are widely used as the main membrane forming materials for MD membrane fabrication.

Over the past 3–5 years, there are many studies reporting the effects of additives in dope solution on the performance of membrane for different membrane process applications. For instance, Zhang et al. [8] reported that the PVDF membrane blended with optimum amount of polyethersulfone (PES) was able to improve the anti-fouling property of pristine PVDF membrane without deteriorating its rejection performance. According to Wang et al. [9] and Bonyadi and Chung [10], the addition of non-solvent additive, i.e. ethylene glycol (EG), tended to enhance the pore size distribution and create ultra-thin skin layer, leading to the enhancement of the permeate flux production.

In general, the major driving force for the separation of feed solution in MD process is the thermal driving force as induced by the difference in transmembrane solution temperature. Recently, there are rising attentions from the researchers to investigate the integration of MD process with renewable energy such as solar energy to substitute the energy sources in heating up the feed solutions [11–15]. Several researchers had validated the viability of the solar-driven MD and concluded that the system is able to produce a substantial amount of permeate flux under prolonged sampling time. In the meantime, few notable solar-driven MD investigations such as the success of MEDESOL (Seawater Desalination by Innovative Solar-powered Membrane Distillation System) under the support of European Commission under sixth framework project had further strengthened the viability of integrating MD with renewable energy in desalting seawater [15].

The main purpose of this work is to fabricate and characterize PVDF membranes blended with different types of additives, i.e. EG and PES, for MD applications. Prior to MD testing, the fabricated membranes were characterized with respect to surface and cross-sectional morphology, pore size, porosity, and hydrophobicity. In the DCMD experiments, the performance of the fabricated membranes was evaluated with respect to permeability and NaCl rejection under various operating conditions. The membrane performance stability test was also conducted under prolonged sampling period in order to assess the potential of this membrane in MD process.

2. Experimental

2.1. Materials

PVDF in pellet form (Kynar 740) obtained from Arkema Inc., Philadelphia, USA and 1-methyl-2-pyrrolidone (NMP, >99.5%) from Sigma Aldrich were used as main membrane forming material and solvent, respectively. EG and PES purchased from Sigma Aldrich and Amoco Chemicals, respectively, were used as additives during dope solution preparation and their chemical structures are shown in Fig. 1. Sodium chloride (NaCl, > 99.5%) from Prochem, was used to prepare 3.5 wt% NaCl feed solution by dissolving the powder salt in distilled water.

2.2. Dope preparation

Table 1 shows the composition of three dope solutions together with their viscosity data that were used to fabricate hollow fiber MD. After all the components were added into the solvent, the dope solutions were continuously stirred for at least 24 h in order to produce a homogenous mixture. Prior to spinning

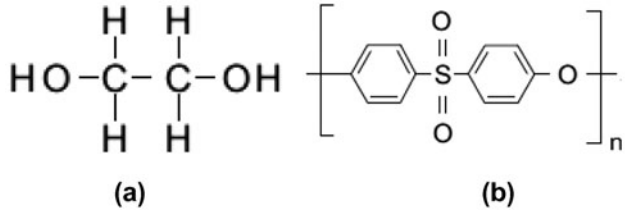

Fig. 1. Molecular structure of (a) ethylene glycol and (b) polyethersulfone.

Table 1
Composition of membrane dope solution

Membrane	PVDF (wt%)	NMP (wt%)	EG (wt%)	PES[a] (wt%)	Viscosity (cP)
PVDF	18	82	–	–	2,367
PVDF–EG	18	76	6	–	2,886
PVDF–EG–PES	18	76	6	5	5,777

[a]The amount of PES added was based on the total weight of PVDF in the dope solution.

process, the dope solutions were degassed using ultrasonic to remove any bubbles that might be trapped within the solution during dope preparation.

2.3. Preparation of hollow fiber membrane

Table 2 summarizes the spinning conditions of hollow fiber membrane fabrication which is based on dry/wet phase inversion method. In this work, prior to membrane module preparation, the as-spun hollow fiber membranes were soaked in water for three days in order to completely remove residual solvent from the membrane matrix. The membranes were then naturally dried at room temperature before use. For detailed description of the spinning process, one can refer to our previous published work [16].

2.4. Membrane characterization

The morphology of the membranes was examined using HITACHI S3400N scanning electron microscope (SEM) to obtain the cross sectional, inner, and outer surface images. Prior to SEM analysis, membrane samples were first immersed into the liquid nitrogen for cryogenic cracking followed by attachment onto a sample holder by carbon tape. The samples were then coated with a thin layer of gold using sputter coater machine (SC7620, Emitech, UK) to enhance its electronic conductivity during sample analysis. The pore size was measured based on the SEM image using Java-based image software, and pore size distribution was plotted by spreadsheet application program.

Table 2
Spinning conditions of hollow fiber membrane fabrication

Parameter	Value
Dope extrusion rate (ml/min)	4.5
Spinneret OD/ID (mm/mm)	1.3/0.6
Bore liquid	Distilled water
Bore liquid temperature (°C)	25
Bore liquid flow rate (ml/min)	2
External coagulant	Tap water
External coagulant temperature (°C)	25
Air gap distance (cm)	10
Room relative humidity (%)	55 ± 5

The membrane porosity, ε, was determined by gravitational method which defined the ratio of the pore volume to the total volume of the porous membrane [17]. For each membrane sample, the dry membrane was first weighted (W_2) followed by the immersion of the membrane into 2-butanol (Fisher Scientific, >99%) solution for 2 h. After 1 h of drying, the weight of the wetted membrane was measured again W_1 in order to determine membrane porosity, ε, as expressed in the following equation.

$$\varepsilon = \frac{(W_1 - W_2)/\rho_W}{(W_1 - W_2)/\rho_W + W_2/\rho_b} \times 100\,\% \quad (1)$$

where W_1 is the weight of the wetted membrane (g), W_2 is the weight of dry membrane (g), ρ_W is the density of 2-butanol (0.81 g cm^{-3}), and ρ_b is the density of PVDF (1.78 g cm^{-3}). For each membrane sample, the measurement was repeated for three times to ensure the reproducibility of the data.

The determination of the degree of membrane hydrophobicity on the other hand was performed in accordance to sessile drop technique (Ramé-Hart Contact Angle Goniometer 250, USA) with the use of DI water as the droplet. At least 10 different spots on the same membrane sample were analyzed to yield the average result. To perform liquid entry pressure (LEP) (also known as wetting pressure) analysis, a test module filled with DI water was required in which five unit of hollow fiber membranes were attached at the bottom of the test module while the other end was connected to a diaphragm pump [18,19]. During the test, the membranes were first pressurized by a slight applied pressure of 0.3 bar to the feed solution for 10 min for degasification. Then, the pressure was increased by a stepwise rate of 0.1 bar, until the first drop of DI water detected on the surface of membrane sample. The corresponding pressure applied to the

membrane in which the first drop of water is detected is considered as LEP. At least three measurements were performed to yield the membrane LEP.

2.5. Experimental setup

The MD experiment was conducted to evaluate the performance of the membranes made of different dope formulations under various operating temperatures and flow rates [20]. Fig. 2 illustrates the setup of the DCMD system used in this study. A predetermined amount of hollow fiber membranes with same effective membrane length was placed within a membrane module with both ends of the module sealed by epoxy resin. The DCMD system was designed to have two circulating streams, i.e. hot stream was fed through the shell-side while cold stream was circulated through the lumen-side of the hollow fiber membrane in counter-current flow. The experiments were carried out under different feed temperatures (40–55 °C) while the inlet temperature of the cold water was kept constant at 18 °C. Both solution temperatures were controlled using coiled heater (HTS-1003, LMS, Japan) and chiller (CA-1112CE, Eyela, Japan), respectively.

The permeate flux of the membranes, J, was calculated using the equation which is similar to [21],

$$J = \frac{\Delta W}{A\Delta t} \tag{2}$$

where J is the permeate flux (kg/m h), ΔW is the difference between the initial and final permeate weight (kg), A is the effective surface area of the membrane (m), and Δt is the sampling time (h).

The rejection, R(%), of NaCl on the other hand was determined using Eq. (3) [21].

$$R = \frac{C_f - C_p}{C_f} \tag{3}$$

where C_f and C_p are the NaCl concentration (ppm) in the feed and permeate solution, respectively.

3. Results and discussion

3.1. Properties of hollow fiber membranes

Fig. 3 presents the SEM images of PVDF membranes prepared with and without additives. As shown in Fig. 3(a), finger-like structure was developed on the inner and outer layer of the pristine PVDF membrane and these two layers of finger-like structures were separated by a sponge-like intermediate layer. The formation of thin selective layer on the inner and outer layer of membrane was due to the strong interaction between the NMP solvent and water (from coagulation bath), leading to immediate solidification on membrane surface (both inner and outer). Because of the thin selective layer formed, the diffusion rate of NMP and water tends to reduce which allows the finger-like layer to form [22]. Comparing the pristine PVDF membrane with the modified PVDF membranes, as shown in Fig. 3(b) and (c), it can be clearly seen that the structure of the pristine PVDF membrane was altered upon addition of additives into the dope solution. With the introduction of EG into PVDF membrane, it is found that irregular size of microvoids was formed at the intermediate layer of membrane along with the decrease in the size of finger-like structure at the inner and outer layer of membrane. This is due to the decrease in the solvent and non-solvent exchange rate during phase inversion process resulting from increased dope viscosity upon EG addition (see Table 1) [23,24]. Interestingly, significant changes in the cross section of PVDF–EG membrane were observed by incorporating additional polymeric material, i.e. PES into PVDF–EG membrane matrix. It is found that irregular size of microvoids existed at intermediate layer of membrane was suppressed by the two-layer finger-like structure extended from the inner and outer layer of membrane. These two layers of finger-like structure were separated only by a thin spongy-like structure as shown in Fig. 3(c). This structural formation might be explained by the relatively poor miscibility between PVDF and PES polymer in the dope in accordance to solubility parameter [25]. In principle, the presence of PVDF and PES polymer

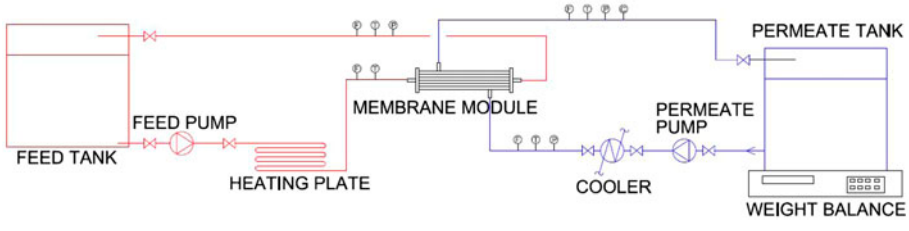

Fig. 2. DCMD setup apparatus.

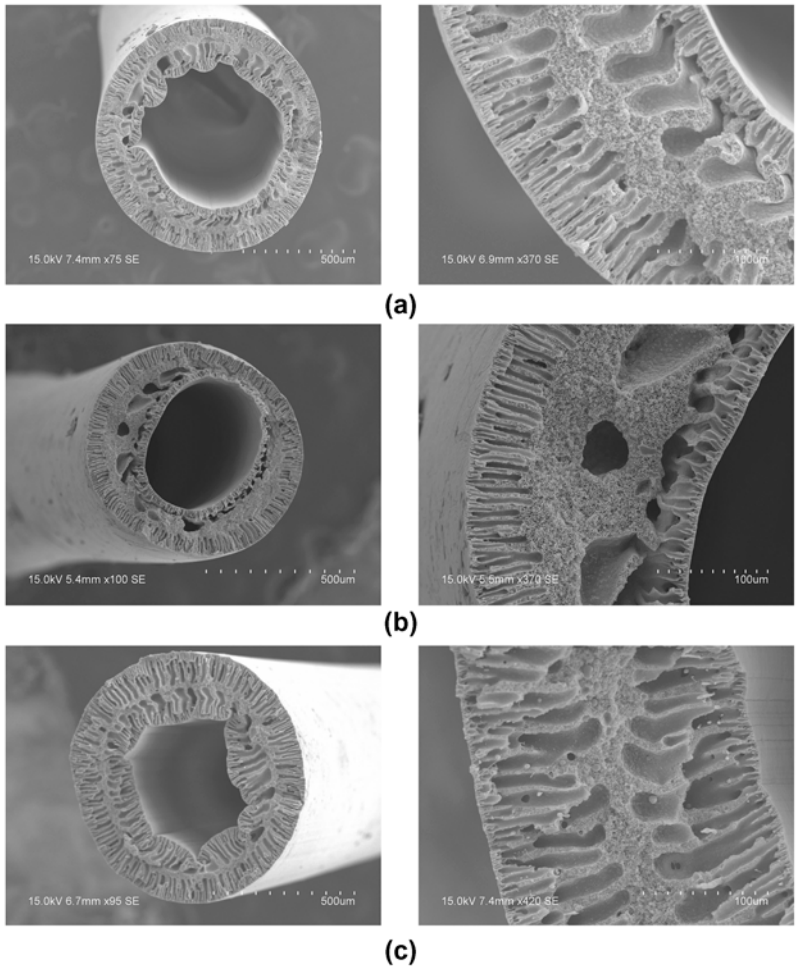

Fig. 3. Cross-sectional view of hollow fiber membrane for MD process, (a) PVDF, (b) PVDF–EG and (c) PVDF–EG–PES.

in the dope solution is thermodynamically incompatible due to the higher solubility parameter of PVDF (15.1 $(cal/cm^2)^{1/2}$) than PES (11.19 $(cal/cm^2)^{1/2}$). This, as a consequence, induces rapid phase separation resulted from faster solvent and non-solvent exchange rate, even though the dope solution is significantly more viscous than the dope of PVDF and PVDF–EG prepared [26].

Table 3 summarizes the properties of all the PVDF membranes prepared from different additives. With respect to membrane wall thickness and inner skin layer thickness, it is found that both thicknesses were decreased by introducing EG into the pristine PVDF membrane. Further introducing PES into the PVDF–EG membrane system would cause the wall thickness and skin layer thickness continued to decrease. The decrease in thickness is strongly linked to better permeate flux during MD process following the decrease in water vapor transport resistance [27]. In addition to the change in membrane thickness, the pore dimension of PVDF membrane was also reported to change upon addition of additive. It is found that the mean pore size of PVDF membranes blended with additives was relatively larger in comparison to the pristine PVDF membrane. With respect to the degree of hydrophobicity, the presence of hydrophilic EG in the pristine PVDF membrane was reported to reduce slightly membrane hydrophobicity by decreasing the water contact angle value from 88° to 82°. Although the water contact angle value of the PVDF–EG membrane was able to increase to 85° upon addition of PES, the membrane hydrophobicity was still relatively lower compared to the pristine PVDF membrane. In addition, it is reported that the LEP of the fabricated membranes was increased in the order of PVDF < PVDF–EG < PVDF–EG–PES with their LEP values falling within the range of 3.5–4.0 bar. Considering the low-operating pressure (i.e. 1 bar) employed in this

Table 3
Characteristics of fabricated hollow fiber membranes

Membrane	PVDF	PVDF–EG	PVDF–EG–PES
Internal diameter (μm)	500	450	400
Wall thickness (μm)	280	230	200
Lumen surface skin thickness (μm)	10 ± 1.23	7 ± 0.75	3 ± 0.37
Mean pore size (μm)	0.25	0.45	0.35
Porosity (%)	80 ± 1.25	60 ± 2.25	70 ± 0.75
Contact angle (°)	88 ± 0.60	82 ± 5.60	85 ± 0.20
LEP (bar)	3.50	3.70	4.00

work for MD process, it is unlikely that pore wetting will occur during the separation process.

3.2. Performance of membrane in DCMD of 3.5 wt% NaCl solution

3.2.1. Effect of feed inlet temperature on membrane permeate flux

Fig. 4 shows the effect of feed inlet temperature on the permeate flux of PVDF membranes blended with and without additives. As can be seen, the permeate flux of membranes was proportionally dependent on the temperature difference in which the higher the feed inlet temperature, the greater the permeate flux produced. This phenomenon can be explained by the increase in vapor pressure in the feed solution following an increase in feed solution temperature, creating greater driving force for water molecules to vaporize. Of the three types of PVDF membranes tested, it is found that the PVDF–EG–PES membranes demonstrated the highest permeate flux followed by PVDF–EG and pristine PVDF membrane. The highest permeate flux achieved by PVDF–EG–PES membrane could be mainly due to its smallest skin layer thickness coupled with relatively large pore size. For PVDF membrane, it is observed that the relatively large skin layer thickness and small mean pore size are the main factors causing the lowest permeate flux produced as evidenced in Fig. 4. Since PVDF–EG–PES is the best performing membrane in terms of permeate flux, the performance of the membrane will be further investigated under different process conditions in the following section.

3.2.2. Effect of feed and permeate flow rate on membrane permeate flux

In this section, two important parameters, i.e. feed and permeate flow rate, were studied using PVDF–EG–PES membrane to determine the optimum flow rate of membrane during MD application. Fig. 5

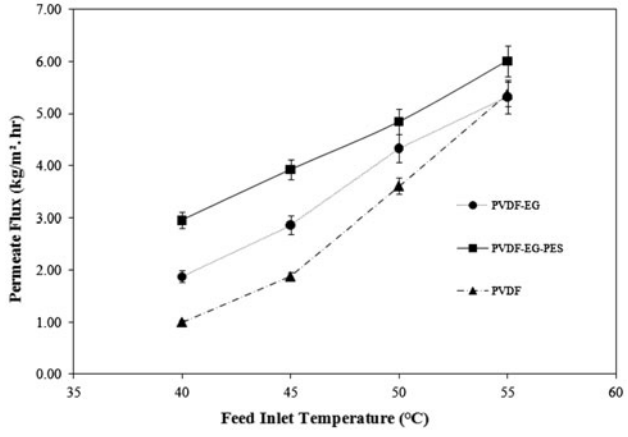

Fig. 4. Permeate flux of PVDF membranes as a function of feed inlet temperature (conditions: permeate temperature: 18°C, feed flow rate: 0.3 L/min, and permeate flow rate: 0.3 L/min).

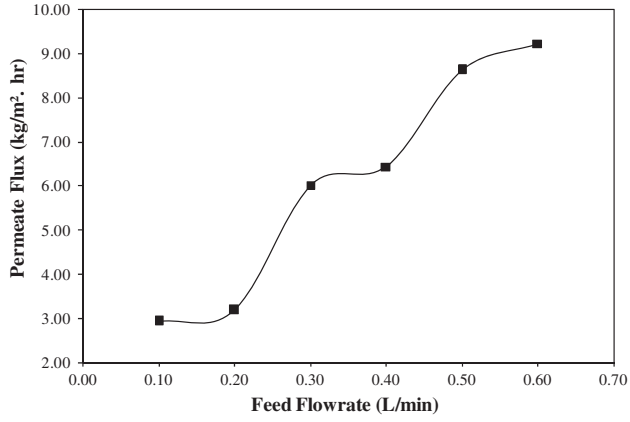

Fig. 5. Permeate flux of PVDF–EG–PES membrane as a function of feed flow rate (conditions: feed inlet temperature = 55°C, permeate inlet temperature = 18°C, and permeate flow rate = 0.3 L/min).

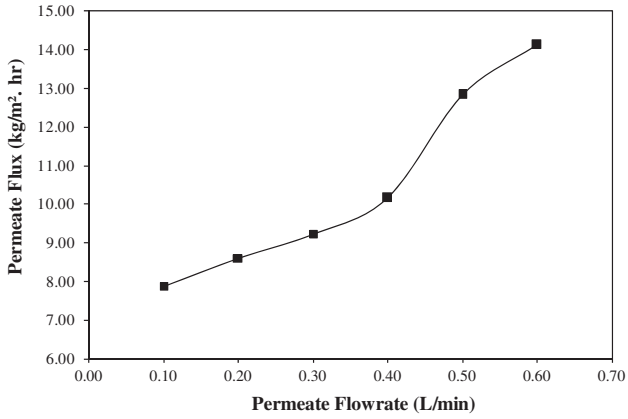

Fig. 6. Permeate flux of PVDF–EG–PES membrane as a function of permeate flow rate (conditions: feed inlet temperature = 55˚C, permeate inlet temperature = 18˚C, and feed flow rate = 0.6 L/min).

shows the effect of feed flow rate on the permeate flux of PVDF–EG–PES membrane. As can be seen, the permeate flux was dependent on the feed flow rate of the MD process. Results show that the flux increment was less significant when membrane was operated at low flow rate of feed stream (0.1–0.2 L/min) compared with the feed flow rate higher than 0.4 L/min. Overall, the permeate flux of membrane was increased threefold from around 3 to >9 kg/m^2 h with increasing the feed flow rate from 0.1 to 0.6 L/min. The significant flux increment can be attributed to the increase in heat transfer coefficient of feed stream flowing at higher flow rate which results in reduction of temperature polarization on the feed side [28,29]. In principle, the temperature at the membrane surface is in close proximity to the bulk feed temperature when feed solution is at high solution flow rate [28,29]. Similar increasing trend was also observed in Fig. 6 when the flow rate of permeate flow solution was increased from 0.1 to 0.6 L/min. Compared to the permeate flux achieved by membrane at flow rate of 0.1 L/min, the permeate flux was significantly improved (approximately 180%) when the permeate flow rate was increased to 0.6 L/min. However, it must be pointed out that high flow rate of stream tends to increase the transmembrane pressure, which is likely to exceed the membrane LEP and further deteriorates permeate quality [1,28,29].

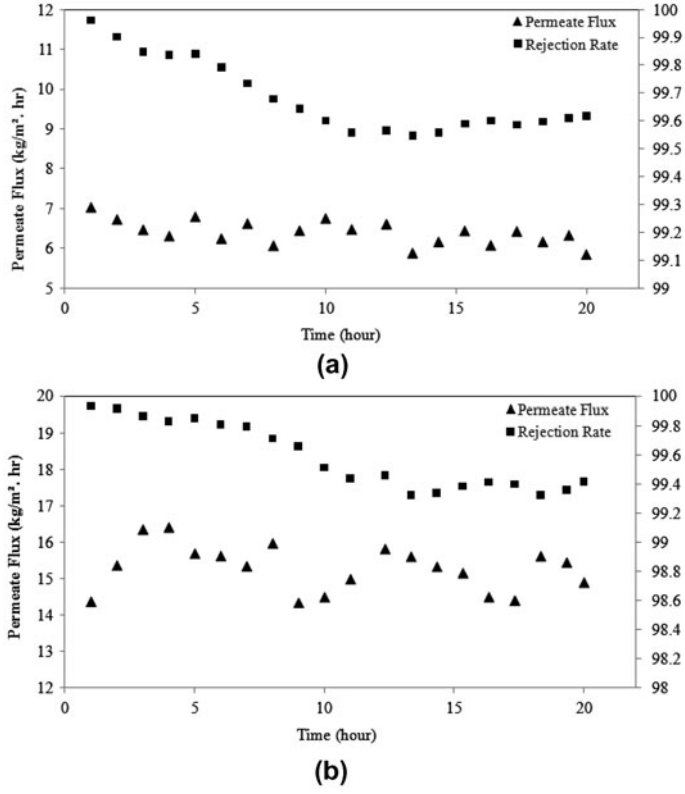

Fig. 7. Stability of PVDF–EG–PES membrane performance as a function of time with contact feed inlet temperature (55˚C) and permeate inlet temperature (18˚C) at different stream flow rates, (a) 0.3 L/min feed flow rate and 0.3 L/min permeate flow rate, and (b) 0.6 L/min feed flow rate and 0.6 L/min permeate flow rate.

3.2.3. Stability of membrane performance under prolonged experimental period

Fig. 7 shows the stability of membrane performance with respect to permeate flux and NaCl rejection as a function of time at different feed and permeate flow rates. As can be seen, the permeate flux of membrane tested at 0.3 L/min feed flow rate and 0.3 L/min permeate flow rate was relatively lower in comparison to the same membrane tested at higher feed and permeate flow rate. The mean permeate flux of membrane at lower flow rate was reported to be around 6.4 $kg/m^2 h$ while it was 15.3 $kg/m^2 h$ at higher flow rate. The enhancement of permeate flux can be mainly attributed to the increase of heat transfer coefficient due to the raise of feed and permeate flow rate, leading to the reduction of temperature polarization [25,27]. With respect to salt separation efficiency, it is reported that only a slight decrease in salt rejection was recorded throughout the entire experimental period. Regardless of stream flow rate, the PVDF–EG–PES membrane was able to consistently produce high quality of water by rejecting at least 99.3% of the NaCl in the feed stream. The insignificant drop in salt rejection (<1.0%) during 20 h continuous separation process indicated the excellent performance stability of membrane in MD process in producing clean water.

4. Conclusions

In this study, three hydrophobic hollow fiber membranes were fabricated using PVDF dope solutions consisting of different additives. The performances of membrane were assessed with respect to permeate flux and NaCl rejection using DCMD system. The morphological study shows that with addition of EG into the PVDF dope solution, the morphology of pristine PVDF membrane has been altered from a finger-like layer with a sponge-like intermediate layer to an irregular size of microvoids at the intermediate layer of membrane. On the other hand, the finger-like structure was extended from both inner and outer layer of membrane and separated by a thin spongy-like structure upon addition of EG–PES. In addition, the membranes blended with additives tended to exhibit smaller lumen surface skin thickness and larger pore size in comparison to pristine PVDF membrane, making them to have greater permeate flux during separation process.

The fabricated membranes were tested using DCMD system and their performances were assessed under different operating conditions. Results show that PES–EG–PES membrane was the best-performing membrane in terms of water permeability. Further investigations also revealed that the water flux of membrane varied depending on feed inlet temperature and flow rate of feed and permeate stream. With respect to performance stability, it is reported that the membrane was able to achieve average flux of 15.3 $kg/m^2 h$ throughout the 20 h experimental period with NaCl rejection maintained at between 99.9 and 99.3%.

Acknowledgements

The authors would like to thank Universiti Tunku Abdul Rahman for providing financial support under Universiti Tunku Abdul Rahman Research Grant (Vote no: 6200/C30).

References

[1] M. Bourawi, Z. Ding, R. Ma, M. Khayet, A framework for better understanding membrane distillation separation process, J. Membr. Sci. 285 (2006) 4–29.
[2] K.W. Lawson, D.R. Lloyd, Membrane distillation, J. Membr. Sci. 124 (1997) 1–25.
[3] M. Tomaszwska, Membrane distillation – Examples of applications in technology and environmental protection, Pol. J. Environ. Stud. 9 (2000) 27–36.
[4] A.K. Manna, M. Sen, A.R. Martin, P. Pal, Removal of arsenic from contaminated groundwater by solar-driven membrane distillation, Environ. Pollut. 158 (2010) 805–811.
[5] S. Yarlagadda, V.G. Gude, L.M. Camacho, S. Pinappu, S.G. Deng, Potable water recovery from As, U, and F contaminated ground waters by direct contact membrane distillation process, J. Hard. Mater. 192 (2011) 1388–1394.
[6] D. Qu, J. Wang, D.Y. Hou, Z.K. Luan, B. Fan, C.W. Zhao, Experimental study of arsenic removal by direct contact membrane distillation, J. Hard. Mater. 163 (2009) 874–879.
[7] Z.W. Ding, L.Y. Liu, Z.M. Li, R.Y. Ma, Z.R. Yang, Experimental study of ammonia removal from water by membrane distillation (MD): The comparison of three configurations, J. Membr. Sci. 286 (2006) 93–103.
[8] M.G. Zhang, Q.T. Nguyen, Z.H. Ping, Hydrophilic modification of poly (vinylidene fluoride) microporous membrane, J. Membr. Sci. 327 (2009) 78–86.
[9] K.S. Wang, T.S. Chung, M. Gryta, Hydrophobic PVDF hollow fiber membranes with narrowpore size distribution and ultra-thin skin for the freshwater production through membrane distillation, Chem. Eng. Sci. 63 (2008) 2587–2594.
[10] S. Bonyadi, T.S. Chung, Highly porous and macrovoid-free PVDF hollow fiber membranes for membrane distillation by a solvent-dope solution co-extrusion approach, J. Membr. Sci. 331 (2009) 66–74.
[11] H. Chang, G.B. Wang, Y.H. Chen, C.C. Li, C.L. Chang, Modeling and optimization of a solar driven membrane distillation desalination system, Renew. Energ. 35 (2010) 2714–2722.

[12] T.C. Chen, C.D. Ho, Immediate assisted solar direct contact membrane distillation in saline water desalination, J. Membr. Sci. 358 (2010) 122–130.
[13] X.Y. Wang, L. Zhang, H.J. Yang, H.L. Chen, Feasibility research of potable water production via solar-heated hollow fiber membrane distillation system, Desalination 247 (2009) 403–411.
[14] J.P. Mericq, S. Laborie, C. Cabassud, Evaluation of systems coupling vacuum membrane distillation and solar energy for seawater desalination, Chem. Eng. J. 166 (2010) 596–606.
[15] J.B. Gálvez, L.G. Rodríguez, I.M. Mateos, Seawater desalination by an innovative solar-powered membrane distillation system: The MEDESOL project, Desalination 246 (2009) 567–576.
[16] W.J. Lau, A.F. Ismail, Theoretical studies on structural and electrical properties of PES/SPEEK blend nanofiltration membrane, Am. Inst. Chem. Eng. J. 55(8) (2009) 2081–2093.
[17] A.L. Ahmad, N. Ideris, B.S. Ooi, S.C. Low, A. Ismail, Synthesis of polyvinlidene fluoride (PVDF) membranes for protein binding: Effect of casting thickness, J. Appl. Polym. Sci. 128 (2012) 3438–3445.
[18] C.A. Smolders, A.C.M. Franken, Terminology for membrane distillation, Desalination 72 (1989) 249–262.
[19] M.C. García-Payo, M. Essalhi, M. Khayet, Effects of PVDF-HFP concentration on membrane distillation performance and structural morphology of hollow fiber membranes, J. Membr. Sci. 347 (2010) 209–219.
[20] S. Al-Obaidani, E. Curcio, F. Macedonio, G. Profio, H. Al-Hinaid, E. Drioli, Potential of membrane distillation in seawater desalination: Thermal efficiency, sensitivity study and cost estimation, J. Membr. Sci. 323 (2008) 85–98.
[21] D.Y. Hou, J. Wang, D. Qu, Z.K. Luan, X.J. Ren, Fabrication and characterization of hydrophobic PVDF hollow fiber membranes for desalination through direct contact membrane distillation, Sep. Purif. Technol. 69 (2009) 78–86.
[22] T.H. Young, L.W. Chen, Pore formation mechanism of membranes from phase inversion process, Desalination 103 (1995) 233–247.
[23] Y. Liao, R. Wang, M. Tian, C.Q. Qiu, A.G. Fane, Fabrication of polyvinylidene fluoride (PVDF) nanofiber membranes by electro-spinning for direct contact membrane distillation, Desalination 425–426 (2013) 30–39.
[24] E. Yuliwati, A.F. Ismail, T. Matsuura, M.A. Kassim, M.S. Abdullah, Characterization of surface-modified porous PVDF hollow fibers for refinery wastewater treatment using microscopic observation, Desalination 283 (2011) 206–213.
[25] L.S. Wu, J.F. Sun, Q.R. Wang, Poly(vinylidene fluoride)/polyethersulfone blend blend membranes: Effects of solvent sort, polyethersulfone and polyvinylpyrrolidone concentration on their properties and morphology, J. Membr. Sci. 285 (2006) 290–298.
[26] D.X. Huang, L. Wang, X.R. Meng, X.D. Wang,L. Zhao, Preparation of PVDF hollow fiber ultrafiltration membrane via phase inversion/chemical treatment method, Desalin. Water Treat. (2013) 1–8.
[27] L. Martínez, J.M. Rodríguez-Maroto, Membrane thickness reduction effects on direct contact membrane distillation performance, J. Membr. Sci. 312 (2008) 143–156.
[28] A. Alkhudhiri, N. Darwish, N. Hilal, Produced water treatment: Application of air gap membrane distillation, Desalination 309 (2013) 46–51.
[29] A. Bahmanyar, M. Asghari, N. Khoobi, Numerical simulation and theoretical study on simultaneously effects of operating parameters in direct contact membrane distillation, Chem. Eng. Process. 61 (2012) 42–50.